White and relaxed noises in optimal velocity models for pedestrian flow with stop-and-go waves

Antoine Tordeux[1,2,*] and Andreas Schadschneider[3]

[1] Jülich Supercomputing Centre, Forschungszentrum Jülich GmbH, Germany
[2] Computer Simulation for Fire Safety and Pedestrian Traffic, Bergische Universität Wuppertal, Germany
[3] Institut für Theoretische Physik, Universität zu Köln, Germany

Abstract

A class of microscopic stochastic models is proposed to describe 1D pedestrian trajectories obtained in laboratory experiments. The class contains continuous first order models that are based on statistically calibrated optimal velocity functions. More specifically we consider a model with an additive white noise and another one where the noise is determined by the inertial Ornstein-Uhlenbeck process. Simulation results show that both stochastic models give a good description of the characteristic relation between speed and spacing (fundamental diagram) and its variability. However, only the inertial noise model can reproduce the observed stop-and-go waves, bimodal speed distributions, and non-zero speed or spacing autocorrelations. This allows to identify minimal microscopic stochastic mechanisms for the emergence of stable traffic waves.

Keywords Pedestrian dynamics, Optimal velocity model, Stochastic noise, Statistical calibration of the parameters, Stop-and-go waves

1 Introduction

The analysis and modelling of pedestrian dynamics has attracted a lot of attention during the last decades [1, 2, 3]. Empirically data have been obtained from experiments in laboratory conditions [4, 5] with software to automatically extract the trajectories from video recordings [6, 7]. These investigations allowed to establish many features of pedestrian dynamics [8], e.g. the unimodal shape of the fundamental flow-density diagram or the presence of stop-and-go waves as characteristics of unidirectional pedestrian streams [8, 9]. Interestingly, these phenomena do not only hold for pedestrians but are also observed for vehicle or bike motion in 1D showing a certain universality in self-driven flows composed of human agents [10].

Numerous models have been developed to understand and analyze the characteristics of self-driven flows [1, 3, 11]. The unimodal shape of the fundamental diagram is already found in simple models like the Asymmetric Simple Exclusion Process (ASEP) [10, 11, 12, 13] where it is related to the exclusion principle. More generally it is well explained microscopically by phenomenological relations between the agent speed and distance spacing to the predecessor usually called *optimal velocity* (OV) function [14]. The relation reflects the tendency to respect safety spacings to avoid collision due to unexpected movements of the predecessor. It is observed for both pedestrians [15] and drivers [16]. The speed in congested traffic seems to be proportional to the distance spacing making the time gap between the agents constant. This constant spacing time can be interpreted as a consequence of the agent/vehicle reaction times (i.e. the sum of the perception, decision and initiation times [17]).

Stop-and-go and clustering effects are self-organization phenomena that have been widely studied [18, 19]. Nonlinear traffic waves and instabilities were the topics of the pioneering papers in the 1950's and early 1960's [20]. Microscopic continuous models defined by systems of differential equations were initially used [21, 22, 23]. This modelling approach is still currently actively developed, see [24]. Inertial OV models belong to the most investigated traffic models [14, 23, 25]. The approach is also used to model pedestrian dynamics [26]. Traffic waves in OV models are analyzed through instability of uniform solutions [27] and mapping to macroscopic soliton equations [28], or chaotic dynamics [29]. Several discrete cellular automata (CA) models are also elaborated to describe non-homogeneous stationary states and traffic waves (see for instance [30, 31, 32, 33] for road traffic CA models). The "slow-to-start" rules, that can been interpreted as a reaction time of drivers out of a jam [34], allows to generate phase separations with

*Corresponding author. Email address: a.tordeux@fz-juelich.de

metastability related to the stability of traffic waves [35, 36]. In a comparable way, a zero-range process for traffic flow with specific backward interaction is used to understand clustering effects [37]. Generally speaking, it seems that the introduction of delays and inertial mechanisms generates instability of the uniform solution and the emergence and stable propagation of stop-and-go waves.

Most of the microscopic models describing nonuniform dynamics are stochastic. CA rules are generically probabilistic while stochastic noises are used in continuous models [38, 39, 40, 41, 42, 43]. In pedestrian models, the noise is used for ambiguous situations (e.g. conflicts) in which two or more behavioral alternatives are equivalent [38] or to model heterogeneous pedestrian behaviors [44]. Few studies have shown that noise plays a major role (see [45] for bidirectional streams and the formation of lanes). For road traffic models, probabilistic distributions of the parameters are also used to model heterogeneous driving styles [46], and stochastic noises are introduced to model perception errors [43] or to switch from a stationary state to another [42]. The use of white noise or time-correlated noises does not impact the global dynamics of second order models [43]. In general, the stochasticity in continuous models does not contribute to the emergence of collective phenomena such as stop-and-go but even tends to disturb it.

In this paper, we show that the introduction of an inertial noise (i.e. defined at second order) in a first order model can impact the dynamics and generate stop-and-go phenomena without requirement of deterministic instabilities. Two stochastic continuous models based on phenomenological OV functions are investigated. A white noise is introduced at the first order within the first model, making the speed non-continuous. The noise is relaxed at the second order through a Langevin equation for the second approach. The speeds are more regular in this last case and a stochastic inertia is introduced. After calibration of the models, we observe by simulation that only the second inertial model is able to give a good description of pedestrian dynamics and notably the stop-and-go wave phenomena. The paper is organized as follows. The stochastic OV models are defined in Sec. 2 and the stability analysis of the deterministic case is done in Sec. 3. The description of the data and the calibration of the models are presented in Sec. 4. The simulation of the models and comparison to the real data are done in Sec. 5. We discuss and interpret the results and statistical values of the parameters in the summary (Sec. 6).

2 Stochastic optimal velocity models

Initially, the optimal velocity model is a second-order model for which the speed is relaxed to an optimal speed depending on the spacing (headway) [14]. The relaxation is determined by an OV function $V : \Delta x \mapsto V(\Delta x)$. Nowadays, any approach based on the OV function is called *OV model* or *extended OV model*. The minimal OV model is [21]

$$\mathrm{d}x_n(t) = V(\Delta x_n(t))\,\mathrm{d}t \tag{1}$$

with $x_n(t)$ the position of agent n at time t and $\Delta x_n(t) = x_{n+1}(t) - x_n(t)$ the distance spacing, $x_{n+1}(t)$ being the position of the first predecessor $n+1$. The uniform solutions are stable in this model if the optimal speed function is increasing which is a natural assumption. The minimal OV model is too simple to reasonably describe wave phenomena. More realistic dynamics are obtained if inertia is introduced through reaction (or relaxation) time parameters. Examples are the *delayed first order OV model* $\mathrm{d}x_n(t+b)/\mathrm{d}t = V(\Delta x_n(t))$ [23], with $b > 0$ the reaction time parameter, or the *ordinary second order OV model* [14]

$$\left\{ \begin{array}{rcl} \mathrm{d}x_n(t) & = & v_n(t)\,\mathrm{d}t, \\ \mathrm{d}v_n(t) & = & \frac{1}{b}\big[V(\Delta x_n(t)) - v_n(t)\big]\mathrm{d}t, \end{array} \right. \tag{2}$$

with $v_n(t)$ the agent speed and $b > 0$ the relaxation time parameter. The OV function calibrates the fundamental diagram while stop-and-go waves can be obtained if the reaction times are sufficiently high so that the stability condition fails. Yet, instability of homogeneous solutions is hard to control. There exists no intrinsic "hard-core" exclusion rule in the delayed first order or second order models. Unrealistic behaviors with collisions or motion backward frequently appear in congested situations [47, 48, 49]. The parameters values giving realistic stop-and-go waves with the deterministic OV models are restricted [50, 51].

Stochastic OV models can be related to discrete models of interacting particle systems [52, 53]. Here, we propose to use stochastic OV models by adding a stochastic noise to the continuous ordinary first order model (1). The noise is centred and stationary, with finite variance. It models other random factors affecting the speed besides the spacing. We use a white noise within the first model. Considering a Wiener process $W(t)$ such that $W(t+s) - W(t)$ is normally distributed with mean zero, variance s, and independent to $W(t)$ for all t and s, the model is

$$\mathrm{d}x_n(t) = V(\Delta x_n(t))\,\mathrm{d}t + \sigma\,\mathrm{d}W_n(t), \tag{3}$$

with σ the amplitude of the white noise. The speed $\mathrm{d}x_n(t)/\mathrm{d}t$ in this model is not continuous and the noise is not autocorrelated. In order to introduce a more regular speed function and a non-vanishing autocorrelation of the noise,

we use the model

$$\left\{ \begin{array}{rcl} \mathrm{d}x_n(t) & = & V(\Delta x_n(t))\,\mathrm{d}t + \varepsilon_n(t)\,\mathrm{d}t, \\ \mathrm{d}\varepsilon_n(t) & = & -\frac{1}{b}\,\varepsilon_n(t)\,\mathrm{d}t + a\,\mathrm{d}W_n(t), \end{array} \right. \tag{4}$$

with a the amplitude of the noise and $b > 0$ the relaxation time parameter. Here the noise is the solution of a Langevin equation. It is a standard Ornstein-Uhlenbeck process, for which the autocorrelation tends to zero exponentially. It is more regular than the white noise (see Fig. 1). Both models (3) and (4) are based on the derivative of the Wiener process. Yet none of them is a Wiener process due to the deterministic mechanism induced by the OV function. The distributions of noise are

- centred normal with variance σ^2 for the white noise model (3);
- centred normal with variance $a^2 b/2$ for the relaxed noise model (4).

Both noises have normal distributions that do not depend on the time (they are stationary) but only the second one is autocorrelated (the use of the relaxation process makes the evolution of the noise smoother).

The Ornstein-Uhlenbeck process is already used in traffic flow to describe the driver attribute, i.e. a parameter specific to each driver, within the generic second order model (GSOM) class [54]. Here it is directly an additive process perturbing the speed. The random oscillations around zero make positive and negative corrections to the optimal speed at random instants with independent increments. This behavior is consistent with action-point traffic models and observations that drivers react at discrete random times [55, 56, 57, 58]. The model (4) is close to the deterministic second order OV model (2). Yet with the stochastic approach, the inertia only affects the noise. As shown in the next section, the uniform solutions are linearly stable in the models (3) and (4) in the deterministic case where $\sigma = a = 0$ as soon as $V(\cdot)$ is strictly increasing. Nevertheless, the trajectories obtained describe nonuniform solutions with stop-and-go waves (see the model (4) in Fig. 2, the simulation details are given in Sec. 5). Yet, contrary to the unstable deterministic approaches, there are no generic problems like collisions and motion backward (see for instance [47, 48, 59] or [60, Chap. 15]). Here, some collisions may occur due to the stochasticity, but their appearances are scarce and not systematic.

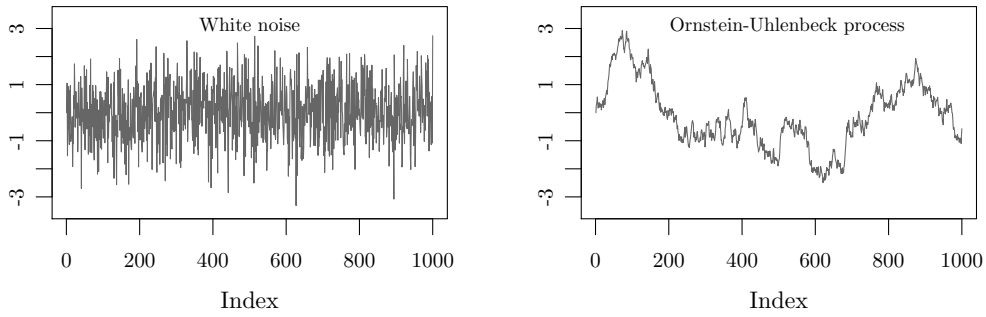

Figure 1: Illustrative example of a white noise (left panel) and the Ornstein-Uhlenbeck process (right panel).

3 Global stability analysis

In this section we analyze the uniform solutions where $x_{n+1}(t) - x_n(t) = d$ and $x_n(t) = x_n(0) + V(d) \cdot t$ for all n and all $t > 0$, with the deterministic OV models on an infinite line with mean spacing $d \geq 0$.

For $\sigma = 0$, the model (3) is the well-known model (1). Denoting $\alpha = V'(d)$, the characteristic equation for the system of dynamical equations linearized around the uniform solution is

$$\lambda + \alpha\big(1 - e^{i\theta}\big) = 0. \tag{5}$$

The uniform solution is globally linearly stable if the real parts of the solutions $\mathrm{Re}(\lambda) = -\alpha(1 - \cos(\theta))$ are strictly negative for all $\theta \in (0, 2\pi)$. This is trivially the case if $\alpha = V'(d) > 0$.

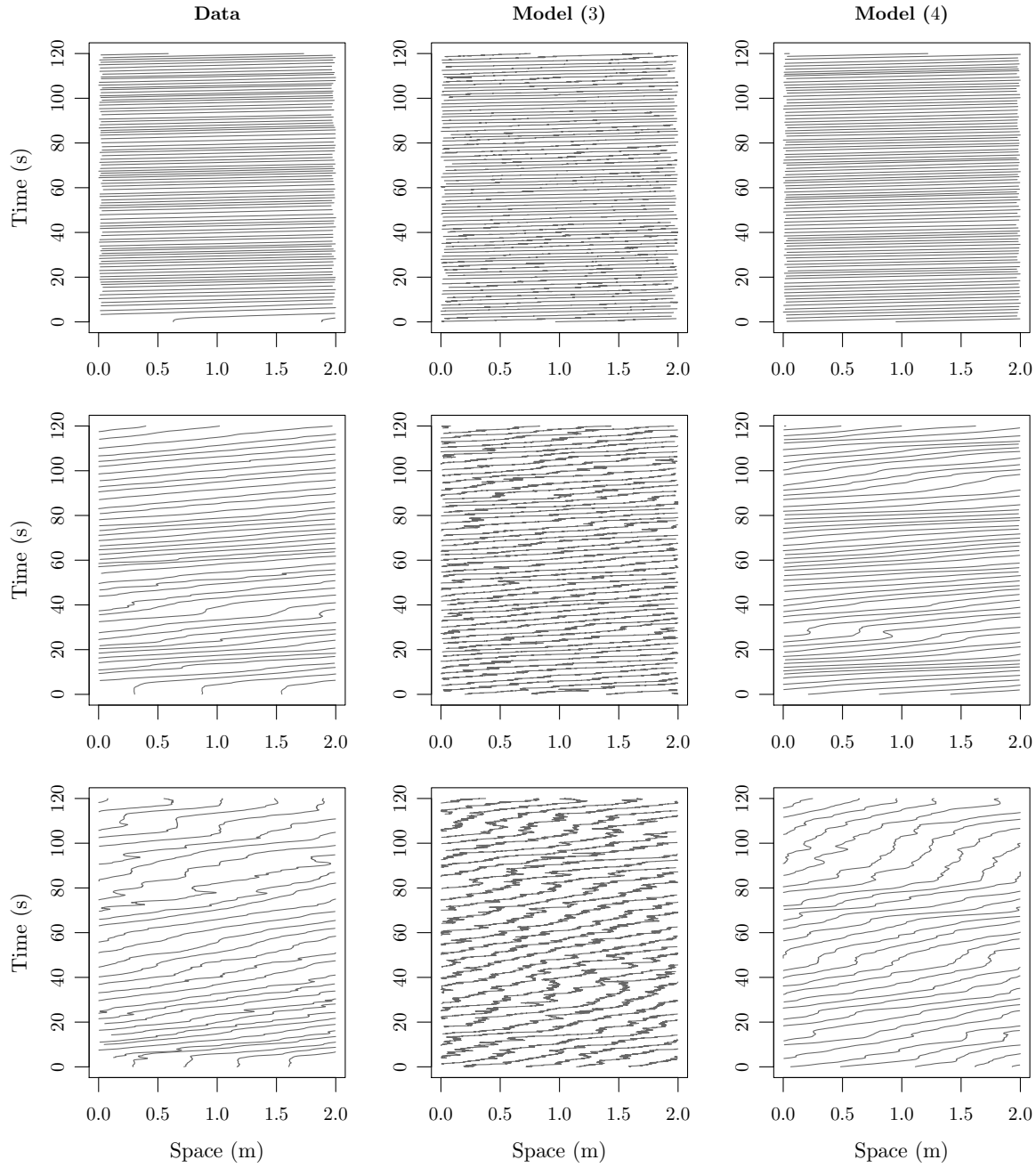

Figure 2: Trajectories on a segment of length 2 m. From top to bottom: 25 (free state), 45 (slightly congested state) and 62 pedestrians (congested state) on the ring of length 27 m. From left to right: Real data and the calibrated models (3) case where $a = 0$ for any value of $b > 0$ as soon as $V(\cdot)$ is strictly increasing. Note that the characteristic equation and the stability conditions remain the same when the reaction time $b > 0$ is a function of the spacing $x_{n+1} - x_n$ if $b'(d) < \infty$.

The linear stability condition of the classical second order OV model (2) is $\alpha b < 1/2$ (see [14]). For the second order model (4) in the deterministic case where $a = 0$, we have $\varepsilon_n(t) = 0$ for all n and all t in the uniform solutions and the characteristic equation for the linear system is

$$\big[\lambda + \alpha\big(1 - e^{i\theta}\big)\big]\big[\lambda + 1/b\big] = 0. \tag{6}$$

From the factorized form of the equation we can directly find that the real parts of the two solutions $\mathrm{Re}(\lambda_1) = -\alpha(1 - \cos(\theta))$ and $\mathrm{Re}(\lambda_2) = -1/b$ are strictly negative if $\alpha = V'(d) > 0$ and $b > 0$ for any $\theta \in (0, 2\pi)$. This proves that,

oppositely to the OV model (2), the model (4) is globally stable in the deterministic case where $a = 0$ for any value of $b > 0$ as soon as $V(\cdot)$ is strictly increasing. Note that the characteristic equation and the stability conditions remain the same when the reaction time $b > 0$ is a function of the spacing $x_{n+1} - x_n$ if $b'(d) < \infty$.

4 Calibration of the parameters

4.1 Empirical data

The data we use to calibrate and evaluate the models are pedestrian trajectories obtained from experiments on a ring with length of 27 m and width of 0.7 m under laboratory conditions [44, 61]. Several experiments with different densities were carried out by varying the number of pedestrians from 14 to 70. In total, 11 different global densities were considered. The initial distribution of the pedestrians was uniform. The trajectories were measured on two segments of length 4 m using the software `PeTrack` [62] with a time resolution of 0.04 s (frame-rate 25 fps). The variables used for the model calibration are the distance spacing and speed

$$\Delta x(t) = x_1(t) - x(t) \qquad \text{and} \qquad v_{\delta t}(t) = \tfrac{1}{\delta t}\big(x(t + \delta t/2) - x(t - \delta t/2)\big), \tag{7}$$

with x_1 the position of the predecessor. The spacings are measured instantaneously while the speeds have to be averaged over time intervals of length $\delta t = k \cdot 0.04$ s, k being a strictly positive even integer (we take $v_{\delta t}(t) = (x(t + \delta t) - x(t))/\delta t$ for $k = 1$). The precision of the speed estimation depends on the value k. Mean value, standard deviation or correlation of speed and spacing remain almost constant when k varies from 1 to 20. Yet we observe for low δt speed oscillations due the steps of the pedestrians. In Fig. 3, the spacing and speed autocorrelations are plotted for $\delta t = 0.04$, 0.4 and 0.8 s. The decrease of the curve for the spacing is regular (see Fig. 3, left panel) while the speed autocorrelation exhibits oscillations for $\delta t = 0.04$ and 0.4 s (see Fig. 3, right panel). The frequency of the oscillation is close to 0.7 s which corresponds to the frequency of pedestrian steps [63]. Further results not presented here show that the frequency depends on the density (it tends to decrease as the density increases). As expected, this phenomenon disappears when the time step is larger than the step frequency. Since stepping is not taken into account in the model, we work in the following with the speed averaged over $\delta t = 0.8$ s to avoid eventual undesired effects of the step frequency.

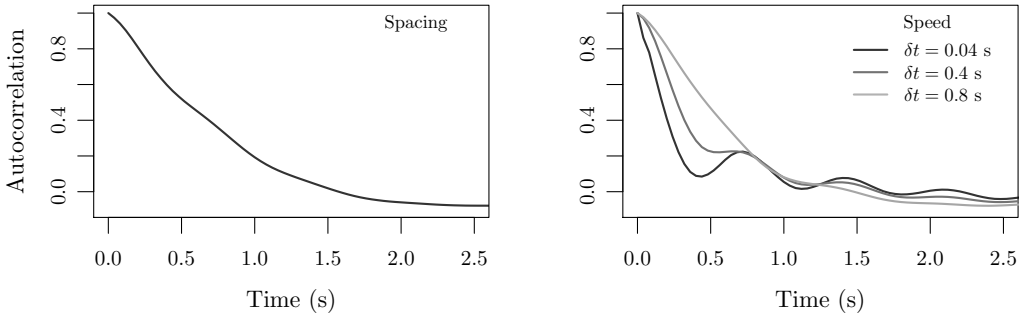

Figure 3: Autocorrelation for the spacing (left panel) and for the speed (right panel). Global sample of observations.

4.2 Estimations of the parameters for the OV function

The OV function models a phenomenological relation between the speed and the spacing. Two main states are classically distinguished: (1) the free state, when the spacing is large and the speed is equal to the maximal desired speed and (2) the congested (or interactive) state, when the spacing is small and the speed depends on the spacing. Both road traffic and pedestrian observations show clear correlations between speed and spacing in congested regimes suggesting that the speed function is initially proportional to the spacing [15, 16]. Therefore, we assume that the OV function is piecewise linear

$$V_p(\Delta x) = \min\big\{v_0, \max\{0, (\Delta x - \ell)/T\}\big\}, \qquad p = (v_0, T, \ell), \tag{8}$$

with v_0 the desired (or maximal) speed, T the time gap and ℓ the longitudinal length of the pedestrian. We propose to estimate these parameters microscopically by using pseudo-independent $K = 5251$ stationary measurements (by

waiting 5 s between each observation and by deleting the beginning and the end of the experiments to avoid transient effects) extracted from the sample of trajectories. We denote the observations by $(\Delta x_k, v_k)$ $(k = 1, \ldots, K)$ where the speed v_k is averaged over $\delta t = 0.8$ s to avoid step frequency effects (see Sec. 4.1). For a given pedestrian k, the residuals $R_k(p)$ of the model are

$$R_k(p) = V_p(\Delta x_k) - v_k. \tag{9}$$

As in [64], the parameters are estimated by minimizing the empirical variance of the residuals

$$\tilde{p} = \arg\min_p \sum_k R_k^2(p), \qquad \tilde{p} = (\tilde{v}_0, \tilde{T}, \tilde{\ell}). \tag{10}$$

This estimation by least squares maximizes the likelihood under the assumption that the residuals are independent and normal, and has in general good properties if the noise repartition is compact. The fitting of the observations and histogram of the residuals are given in Fig. 4. The parameters estimations are: $\tilde{v}_0 = 0.92$ m/s, $\tilde{T} = 1.04$ s and $\tilde{\ell} = 0.34$ m. The $R^2 = 0.78$ of the estimation (the proportion of the variance explained by the model) reveals a good fit of the model. Moreover the distribution of the residuals is relatively compact. The fit can be slightly improved by using sigmoid OV functions with 4 parameters ($R^2 = 0.80$). Note that the parameter values remain approximately the same if we use the instantaneous speed calculated with $\delta t = 0.04$ (we obtain $\tilde{v}_0 = 0.94$ m/s, $\tilde{T} = 1.02$ s, $\tilde{\ell} = 0.34$ m and $R^2 = 0.78$). Therefore the statistical calibration of the parameters is robust to the step frequency of the pedestrian trajectories.

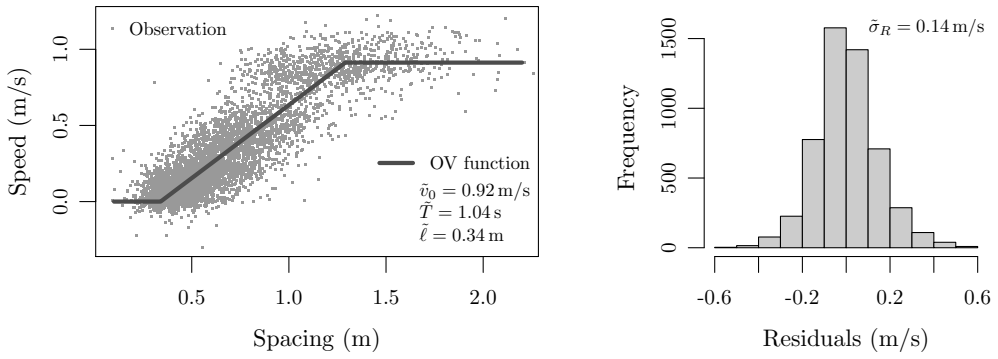

Figure 4: Statistical estimation of the parameters (left panel) and histogram of the residuals (right panel). $\tilde{\sigma}_R$ is the empirical standard deviation of the residuals. $\delta t = 0.8$ s in the calculus of the speed. Global sample of observations.

The parameter estimations are obtained with a sample of $K = 5251$ observations. Some estimations are done with sub-samples of size $K' = 100$ to evaluate the precision of the estimations with the global sample. The histograms of the estimations of 500 sub-samples are presented in Fig. 5. The estimations are relatively precise, even if the sample size is only 100 observations. More than 90% of the estimations belong to the intervals $[0.83\ \mathrm{m/s}, 1.04\ \mathrm{m/s}]$ for the desired speed v_0, $[0.88\ \mathrm{s}, 1.21\ \mathrm{s}]$ for the pedestrian time gap T, and $[0.29\ \mathrm{m}, 0.40\ \mathrm{m}]$ for the diameter ℓ. The global dataset is more than 50 times bigger than the sub-samples. Therefore, we can deduce that the estimations obtained with the global sample are relatively precise.

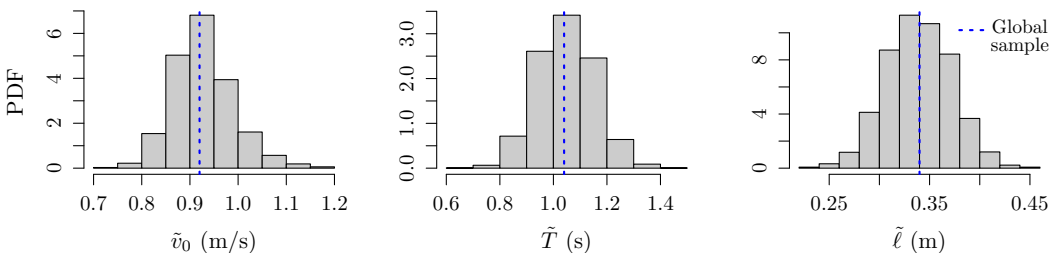

Figure 5: Histogram of the parameter estimations obtained with sub-samples of 100 observations. The vertical dotted lines are the estimations with the global sample of observations.

4.3 Estimations of the parameters for the noise

The empirical estimation of variance of the residuals maximizing the likelihood is $\tilde{\sigma}_R^2 = \frac{1}{K}\sum_k R_k^2(\tilde{p})$. In the models, the difference of the Wiener process $W(t+\delta t) - W_n(t)$ is normally distributed with variance equal to the time step δt for all t. Therefore within the model (3), the estimation of σ is

$$\tilde{\sigma} = \tilde{\sigma}_R\sqrt{\delta t}. \tag{11}$$

For the model (4), the stationary variance of the Ornstein-Uhlenbeck process is $\mathrm{var}(\varepsilon(t)) = a^2 b/2$ while the auto-covariance at time δt is $\mathrm{cov}(\varepsilon(t+\delta t), \varepsilon(t)) = a^2 b e^{-\delta t/b}/2$. Here 'stationary' means that the parameters do not depend on time. This is reasonable with the data since initial and ending observations of transient states are not considered. These relations allow to obtain the estimators for b and a

$$\tilde{b} = -\delta t/\log(\tilde{c}_{\delta t}) \qquad \text{and} \qquad \tilde{a} = \tilde{\sigma}_R\sqrt{2/\tilde{b}} \tag{12}$$

with $\tilde{c}_{\delta t} = \mathrm{cov}(\varepsilon(t+\delta t), \varepsilon(t))/\mathrm{var}(\varepsilon(t))$ the empirical autocorrelation of the process $\varepsilon(t)$. The estimations for all the data are $\tilde{\sigma} \approx 0.13$ ms$^{-1/2}$, $\tilde{b} \approx 4.38$ s and $\tilde{a} \approx 0.09$ ms$^{-3/2}$. Note that the value of the relaxation time b is close to 5 s that is 10 times larger than the reaction (or relaxation) time $\tau \approx 0.5$ s generally used as an input parameter with force-based pedestrian models (see for instance [38], the value is in the order of the measured pedestrian reaction time [65]). The histograms of the estimations obtained with sub-samples of $K' = 100$ observations are plotted in Fig. 6. We observe that more than 90% of the estimations belongs to the intervals $[0.11\ \mathrm{m}^{-1/2}, 0.14\ \mathrm{m}^{-1/2}]$ for the noise amplitude σ, $[0.08\ \mathrm{ms}^{-3/2}, 0.12\ \mathrm{ms}^{-3/2}]$ for the amplitude of the relaxed noise a, and $[2.71\ \mathrm{s}, 6.75\ \mathrm{s}]$ for the relaxation time b. Here again, the estimations obtained are relatively precise, even if the sub-sample size is quite small. Only the parameter b is more fluctuating, with a range of ± 2 s in the 90% confidence interval. Yet the global sample size is approximately 50 times bigger than the one of the sub-samples, making the estimations of the noise parameters with all the data relatively precise.

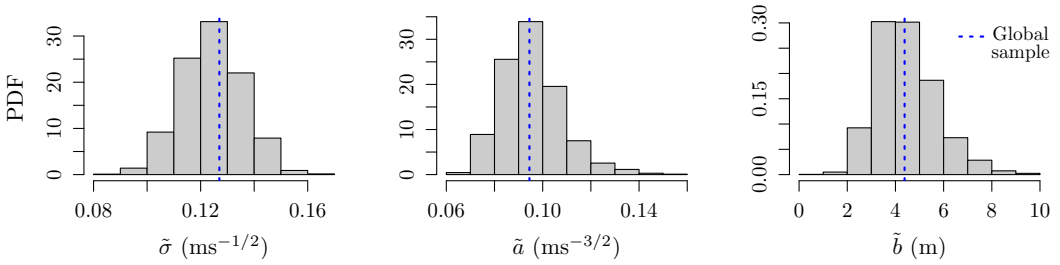

Figure 6: Histogram of the estimations for the parameters of the noise obtained with sub-samples of 100 observations. The vertical dotted lines are the estimations with the global sample of observations.

Estimations by class of spacing show clear relations between the noise parameters and this variable. The results are shown in Fig. 7. We can see for $\tilde{\sigma}$ and $\tilde{b}$ particular uni-modal shapes in the congested phase where $\Delta x \leq \ell + v_0 T \approx 1.3$ m. For the free phase where $\Delta x \geq \ell + v_0$, the values are relatively constant. The shape of the parameter $\tilde{a}$ is more irregular. It will be assumed to be constant for $\Delta x < 0.95$ m and $\Delta x \geq 0.95$ m, respectively, in the simulations.

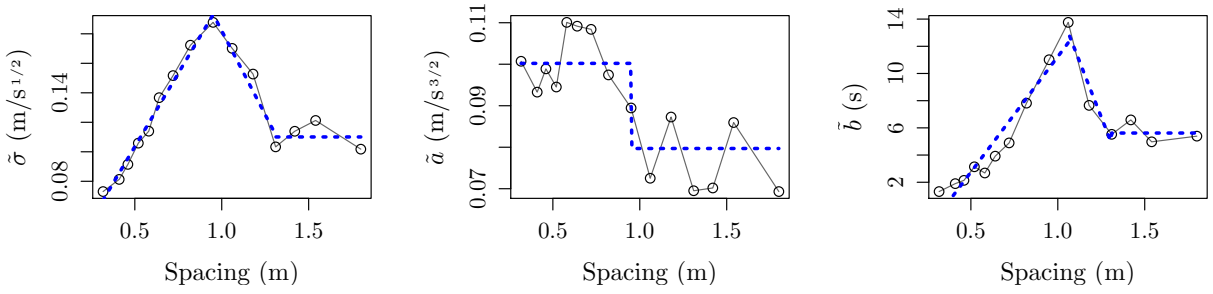

Figure 7: Statistical estimations of the noise parameters by class of spacing. The dotted lines are the linear approximations used in the simulations.

5 Simulation results

In the analysis of complex systems, the *top-down* method consists in calibrating the parameters of a microscopic model in order to reproduce observed macroscopic behavior. It requires knowledge about the relation between the parameter values and the macroscopic properties of the model (i.e. sensitivity analysis). The top-down approach has been mainly used in particle physics where the microscopic particle behavior is unknown (only macroscopic quantities such as the temperature are measured). In this study, the microscopic performances (i.e. the trajectories) are observed and directly used to calibrate the parameters. The macroscopic behaviors are observed by simulation and used to validate, or not, the calibrated models. This *bottom-up* approach allows to control both local and global dynamics.

Here, we evaluate the models (3) and (4) by comparing simulation results to the real data. A similar setup as in the real experiments is reproduced for the simulations (from 14 to 70 pedestrians on a ring of length 27 m with uniform initial configuration). The models are simulated by using explicit Euler-Maruyama schemes [66]. The discretisation of the white noise model (3) is

$$x_n(t+dt) = x_n(t) + dt\, V_{\tilde{p}}(\Delta x_n(t)) + \sqrt{dt}\,\tilde{\sigma}\,\xi_n(t), \tag{13}$$

while the discrete relaxed noise model (4) is

$$\left\{ \begin{array}{rcl} x_n(t+dt) & = & x_n(t) + dt\, V_{\tilde{p}}(\Delta x_n(t)) + dt\,\varepsilon_n(t), \\ \varepsilon_n(t+dt) & = & (1 - dt/\tilde{b})\,\varepsilon_n(t) + \sqrt{dt}\,\tilde{a}\,\xi_n(t), \end{array} \right. \tag{14}$$

with $(\xi_n(t), n, t)$ independent normal random variables. The processes are Makovian chains where the state of the system at time t solely depends on the state at time $t - dt$. The time step dt is set to 10^{-3} s for that the numerical scheme converges and that the discrete solutions Eqs. (13) and (14) are close to the continuous ones Eqs. (3) and (4). The parameter values are the ones given in Sec. 4 (see Figs. 4 and 7). The time step δt for the calculation of the speed is set to 0.8 s to avoid the step effect observed in the data (see Sec. 4.1). Yet, most of the following presented results remain valid for smaller value of this parameter (i.e. for a more precise description of the speed).

The models are firstly evaluated by looking at the mean, standard deviation and correlation of the speed and spacing for the global sample of observations (see Table 1). Both models (3) and (4) present a good fit to the real data. Only the correlation between the speed and predecessor speed with the model (3) is significantly different from the data. Such statement was expected since the speeds are independent random variables within the white noise model.

Variables	Δx			$v_{\delta t}$			Δx^1			$v^1_{\delta t}$		
Data	Real	Model (3)	Model (4)	Real	(3)	(4)	Real	(3)	(4)	Real	(3)	(4)
Mean	0.68	0.67	0.67	0.32	0.31	0.32	0.68	0.67	0.67	0.32	0.31	0.31
Std-dev	0.33	0.33	0.34	0.30	0.29	0.30	0.33	0.32	0.35	0.30	0.29	0.30
Corr. Δx	1	1	1	0.87	0.85	0.87	0.79	0.81	0.76	0.87	0.86	0.87
$v_{\delta t}$	0.87	0.85	0.87	1	1	1	0.85	0.79	0.84	0.96	0.84	0.97

Table 1: Mean, standard deviation (in m and m/s) and correlation for the spacing Δx and speed $v_{\delta t}$ of a pedestrian and his/her predecessor (Δx^1 and $v^1_{\delta t}$) for global sample of observations. $\delta t = 0.8$ s.

The trajectories for 25, 45 and 62 pedestrians are presented in Fig. 2. Some stop-and-go waves propagate when the density increases (see Fig. 2, middle and bottom panels). The trajectories of the white noise model (3) are very irregular, especially for high density levels. Moreover we do not observe stable propagation of stop-and-go waves in this model. The trajectories are qualitatively very similar to the data for any density level of the relaxed noise model (4). Even if the uniform solutions are linearly stable for the model (4) in the deterministic case, the trajectories obtained describe nonuniform solutions with stop-and-go waves. Oppositely to the unstable deterministic approaches, we do not observe the generic collision and motion backward problems (see for instance [47, 48]).

The good fitting of the relaxed model (4) is confirmed when observing the autocorrelation of the speed and spacing (see Fig. 8). The values obtained are underestimated with the model (3), while the fit is reasonable with the model (4). This is especially the case with the speed, for which the autocorrelation vanishes by construction for any time higher that the averaging time $\delta t = 0.8\,s$ with the model (3) (it linearly decreases from one to zero for times smaller than δt due to the moving average). The speed autocorrelation qualitatively decreases exponentially for the data and the model (4).

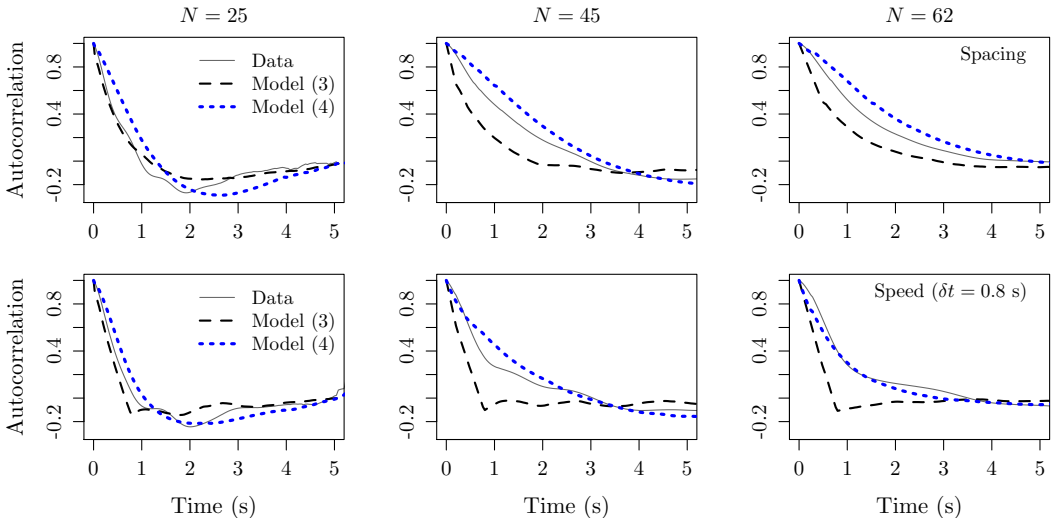

Figure 8: Autocorrelation function for the spacing (top panels) and the speed (bottom panels) for $N = 25$ (free state, left panels), $N = 45$ (slightly congested state, middle panels) and $N = 62$ (congested state, right panels).

The speed distributions in different spacing regimes are plotted in Fig. 9. We observe bimodal distributions for intermediate spacings within the data and model (4) (see Fig. 9, middle panel), corresponding to the presence of stable stop-and-go waves, whereas the distribution is unimodal in the white noise model (3). This observation confirms the necessity of using inertial mechanisms in the models to describe stable traffic waves. This is in agreement with the results obtained for the classical deterministic approaches [14, 27, 51]. Note that further simulations show that this phenomenon does not depend on the value of the time step dt in the numerical scheme, as soon as it is small enough (we observed stop-and-go for dt up to 0.5 s; at least we should have $dt \leq \min\{T, b\}$). Therefore the stop-and-go waves are a characteristic of the continuous model (4) and not a discretisation effect.

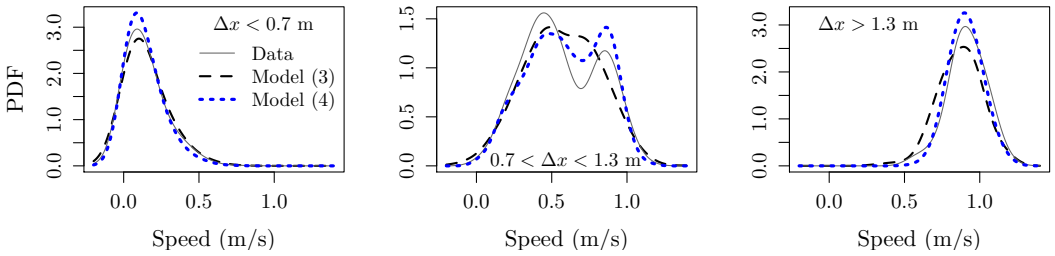

Figure 9: Probability density function of the speed $v_{\delta t}$ with $\delta t = 0.8\,s$ for different regimes of the spacing Δx with the global sample of observations.

6 Conclusion

A class of continuous pedestrian speed (i.e. first order) models based on phenomenological OV functions and stochastic noises is proposed and calibrated with real trajectories. Two models are compared: a white noise and a relaxed one described by the Ornstein-Uhlenbeck process. Both stochastic models give realistic descriptions of pedestrian trajectories. Mean values and correlations of the speed and spacing are relatively well fitted though piecewise linear OV function with three parameters. Yet only the relaxed noise model allows to obtain stop-and-go phenomena at congested density levels with bimodal speed distributions, and non-zero speed and spacing autocorrelations. Additive white noises are not sufficient to describe stable wave phenomena within first order OV models.

As the classical deterministic OV models, inertia and delay mechanisms are used to generate collective waves. Yet the inertia here is stochastic, without deterministic instability of the uniform solution. Also, and oppositely to classical

models, there is no requirement of using nonlinear dynamics to obtain traffic waves within the stochastic OV approach. Moreover, we do not observe the generic problems of collision and motion backward that are unfortunately frequently obtained with the unstable deterministic approaches. The statistical estimation of the relaxation time is close to 5 s for the noisy model, while it is generally an input parameter for the reaction time around 0.5 s for the deterministic Ansatz. Also, the relaxation mechanism of the stochastic approach is not that of the classical models. This makes the inertial stochastic OV model a new minimal way to describe stop-and-go phenomena. For pedestrian dynamics in two dimensions, the speed model has to be completed by a direction model.

Acknowledgement

The authors thank Prof. Michel Roussignol for his help in the formulation of the model (4). A.T. is supported by the project BaSiGo (Bausteine für die Sicherheit von Großveranstaltungen – Safety and Security Modules for Large Public Events) funded by the Federal Ministry of Education and Research (BMBF) Program on 'Research for Civil Security, Protecting and Saving Human Life' under grant number 13N12045. We thank the Deutsche Forschungsgemeinschaft (DFG) for support under the grants Scha 636/9-1 and SE 1789/4-1.

References

[1] D. Helbing. Traffic and related self-driven many-particle systems. *Rev. Mod. Phys.*, 73:1067–1141, 2001.

[2] A. Schadschneider, W. Klingsch, H. Klüpfel, T. Kretz, C. Rogsch, and A. Seyfried. Evacuation dynamics: Empirical results, modeling and applications. *Encyclopedia of Complexity and System Science*, 3:3142–3176, 2009.

[3] A. Schadschneider, D. Chowdhury, and K. Nishinari. *Stochastic Transport in Complex Systems. From Molecules to Vehicles*. Elsevier, Amsterdam, 2010.

[4] W. Daamen and S. Hoogendoorn. Controlled experiments to derive walking behaviour. *Eur. J. Transp. Infrastr. Res.*, 3(1):39–59, 2003.

[5] M. Boltes, J. Zhang, and A. Seyfried. Analysis of crowd dynamics with laboratory experiments. In S. Ali, K. Nishino, D. Manocha, and M. Shah, editors, *Modeling, Simulation and Visual Analysis of Crowds*, volume 11, pages 67–97. Springer New York, 2013.

[6] P. Dollar, C. Wojek, B. Schiele, and P. Perona. Pedestrian detection: An evaluation of the state of the art. *IEEE Trans. Pattern Anal. Mach. Intell.*, 34(4):743–761, 2012.

[7] M. Boltes and A. Seyfried. Collecting pedestrian trajectories. *Neurocomputing*, 100:127–133, 2013.

[8] A. Schadschneider, H. Klüpfel, T. Kretz, C. Rogsch, and A. Seyfried. Fundamentals of pedestrian and evacuation dynamics. In A. Bazzan and F. Klügl, editors, *Multi-Agent Systems for Traffic and Transportation Engineering*, pages 124–154. IGI Global, Hershey, USA, 2009.

[9] A. Seyfried, A. Portz, and A. Schadschneider. Phase coexistence in congested states of pedestrian dynamics. *Lect. Notes Comp. Sc.*, 6350:496–505, 2010.

[10] J. Zhang, W. Mehner, S. Holl, M. Boltes, E. Andresen, A. Schadschneider, and A. Seyfried. Universal flow-density relation of single-file bicycle, pedestrian and car motion. *Phys. Lett. A*, 378(44):3274–3277, 2014.

[11] D. Chowdhury, L. Santen, and A. Schadschneider. Statistical physics of vehicular traffic and some related systems. *Phys. Rep.*, 329(4-6):199–329, 2000.

[12] M.T. Liggett. *Interacting Particle Systems*. Classics in Mathematics. Springer-Verlag, Berlin Heidelberg, 2004.

[13] M. Evans. Phase transitions in stochastic models of flow. In A. Schadschneider, T. Pöschel, R. Kühne, M. Schreckenberg, and D. E. Wolf, editors, *Traffic and Granular Flow'05*, volume 5, pages 447–459, 2007.

[14] M. Bando, K. Hasebe, A. Nakayama, A. Shibata, and Y. Sugiyama. Dynamical model of traffic congestion and numerical simulation. *Phys. Rev. E*, 51(2):1035–1042, 1995.

[15] A. Jelic, C. Appert-Rolland, S. Lemercier, and J. Pettré. Properties of pedestrians walking in line: Fundamental diagrams. *Phys. Rev. E*, 85:036111, 2012.

[16] J. H. Banks. Average time gaps in congested freeway flow. *Transport. Res. A-Pol.*, 37:539–554, 2003.

[17] W. Leutzbach. *An Introduction to the Theory of Traffic Flow*. Springer Berlin, 1988.

[18] T. Li. Nonlinear dynamics of traffic jams. *Physica D*, 207(1-2):41–51, 2005.

[19] G. Orosz, R. E. Wilson, R. Szalai, and G. Stépán. Exciting traffic jams: Nonlinear phenomena behind traffic jam formation on highways. *Phys. Rev. E*, 80(4):046205, 2009.

[20] D. C. Gazis. The origins of traffic theory. *Op. Res.*, 50(1):69–77, 2002.

[21] L. A. Pipes. An operational analysis of traffic dynamics. *J. Appl. Phys.*, 24(3):274–281, 1953.

[22] D. C. Gazis, R. Herman, and R. W. Rothery. Nonlinear follow-the-leader models of traffic flow. *Op. Res.*, 9(4):545–567, 1961.

[23] G. F. Newell. Nonlinear effects in the dynamics of car-following. *Op. Res.*, 9(2):209–229, 1961.

[24] R. E. Wilson and J. A. Ward. Car-following models: Fifty years of linear stability analysis - A mathematical perspective. *Transport. Plan. Techn.*, 34(1):3–18, 2011.

[25] M. Bando, K. Nakanishi, and A. Nakayama. Analysis of optimal velocity model with explicit delay. *Phys. Rev. E*, 58(5):5429–5435, 1998.

[26] A. Nakayama, K. Hasebe, and Y. Sugiyama. Instability of pedestrian flow and phase structure in a two-dimensional optimal velocity model. *Phys. Rev. E*, 71:036121, 2005.

[27] G. Orosz, R. E. Wilson, and G. Stepan. Traffic jams : dynamics and control. *Proc. R. Soc. A*, 368(1957):4455–4479, 2010.

[28] T. S. Komatsu and S.-I. Sasa. Kink soliton characterizing traffic congestion. *Phys. Rev. E*, 52(5):5574–5582, 1995.

[29] L. A. Safonov, E. Tomer, V. V. Strygin, Y. Ashkenazy, and S. Havlin. Delay-induced chaos with multifractal attractor in a traffic flow model. *EPL*, 57(2):151–157, 2002.

[30] M. Schreckenberg, A. Schadschneider, K. Nagel, and N. Ito. Discrete stochastic models for traffic flow. *Phys. Rev. E*, 51:2939–2949, 1995.

[31] S. Krauss, P. Wagner, and C. Gawron. Metastable states in a microscopic model of traffic flow. *Phys. Rev. E*, 55(5):5597–5602, 1997.

[32] W. Knospe, L. Santen, A. Schadschneider, and M. Schreckenberg. Towards a realistic microscopic description of highway traffic. *J. Phys. A*, 33(48):L477, 2000.

[33] B. S. Kerner, S. L. Klenov, and D. E. Wolf. Cellular automata approach to three-phase traffic theory. *J. Phys. A*, 35(47):9971–10013, 2002.

[34] P. Wagner. Modelling traffic flow fluctuations, cond-mat/0411066, 2004.

[35] A. Schadschneider and M. Schreckenberg. Traffic flow models with "slow-to-start" rules. *Ann. Physik*, 6:541–551, 1997.

[36] R. Barlovic, L. Santen, A. Schadschneider, and M. Schreckenberg. Metastable states in cellular automata for traffic flow. *Eur. Phys. J. B*, 5(3):793–800, 1998.

[37] J. Kaupuzs, R. Mahnke, and R. J. Harris. Zero-range model of traffic flow. *Phys. Rev. E*, 72(5):056125, 2005.

[38] D. Helbing and P. Molnár. Social force model for pedestrian dynamics. *Phys. Rev. E*, 51:4282–4286, 1995.

[39] R. Kosiński and A. Grabowski. Langevin equations for modeling evacuation processes. *Acta. Phys. Pol. B Proc. Suppl.*, 3(2):365–376, 2010.

[40] M. Burger, M. Di Francesco, P.A. Markowich, and M.T. Wolfram. Mean field games with nonlinear mobilities in pedestrian dynamics. *DCDS*, 19(5):1311–1333, 2014.

[41] D. Jost and K. Nagel. Probabilistic traffic flow breakdown in stochastic car following models. In S. P. Hoogendoorn, S. Luding, P. H.L. Bovy, M. Schreckenberg, and D. E. Wolf, editors, *Traffic and Granular Flow '03*, pages 87–103. Springer Berlin Heidelberg, 2005.

[42] E. Tomer, L. Safonov, and S. Havlin. Presence of many stable nonhomogeneous states in an inertial car-following model. *Phys. Rev. Lett.*, 84(2):382–385, 2000.

[43] M. Treiber, A. Kesting, and D. Helbing. Delays, inaccuracies and anticipation in microscopic traffic models. *Physica A*, 360(1):71–88, 2006.

[44] A. Portz and A. Seyfried. Analyzing stop-and-go waves by experiment and modeling. In R.D. Peacock, E.D. Kuligowski, and J.D. Averill, editors, *Pedestrian and Evacuation Dynamics 2010*, pages 577–586, 2011.

[45] D. Helbing, I.J. Farkas, and T. Vicsek. Freezing by heating in a driven mesoscopic system. *Phys. Rev. Lett.*, 84:1240–1243, 2000.

[46] S. Ossen, S. P. Hoogendoorn, and B. G. Gorte. Interdriver differences in car-following : A vehicle trajectory based study. *Transport. Res. Record*, 1965:121–129, 2008.

[47] L. C. Davis. Modifications of the optimal velocity traffic model to include delay due to driver reaction time. *Phyica. A*, 319(0):557–567, 2003.

[48] R. E. Wilson, P. Berg, S. Hooper, and G. Lunt. Many-neighbour interaction and non-locality in traffic models. *Eur. J. Phys. B*, 39(3):397–408, 2004.

[49] A. Tordeux and A. Seyfried. Collision-free nonuniform dynamics within continuous optimal velocity models. *Phys. Rev. E*, 90:042812, 2014.

[50] K. Nakanishi. Multibunch solutions of the differential-difference equation for traffic flow. *Phys. Rev. E*, 62(3):3349–3355, 2000.

[51] I. Gasser, T. Seidel, G. Sirito, and B. Werner. Bifurcation analysis of a class of "car following" traffic models II: variable reaction times and aggressive drivers. *Bull. Inst. Math. Acad. Sin.*, 2(2):587–607, 2007.

[52] M. Kanai, K. Nishinari, and T. Tokihiro. Stochastic optimal velocity model and its long-lived metastability. *Phys. Rev. E*, 72:035102, 2005.

[53] M. Kanai, K. Nishinari, and T. Tokihiro. Analytical study on the criticality of the stochastic optimal velocity model. *J. Phys. A*, 39(12):2921–2935, 2006.

[54] M. M. Khoshyaran and J.-P. Lebacque. A stochastic macroscopic traffic model devoid of diffusion. In C. Appert-Rolland, F. Chevoir, P. Gondret, S. Lassarre, J.-P. Lebacque, and M. Schreckenberg, editors, *Traffic and Granular Flow '07*, pages 139–150. Springer Berlin Heidelberg, 2009.

[55] E. Todosiev. *The action point model of the driver-vehicle system*. PhD thesis, Ohio State University, 1963.

[56] P. Wagner. How human drivers control their vehicle. *Eur. Phys. J. B*, 52(3):427–431, 2006.

[57] P. Wagner and I. Lubashevsky. Empirical basis for car-following theory development. Technical report, German Aerospace Center, Germany, 2006.

[58] A. Zgonnikov, I. Lubashevsky, S. Kanemoto, T. Miyazawa, and T. Suzuki. To react or not to react? Intrinsic stochasticity of human control in virtual stick balancing. *J. R. Soc. Interface*, 11:2014063, 2014.

[59] M. Chraibi, T. Ezaki, A. Tordeux, K. Nishinari, A. Schadschneider, and A. Seyfried. Jamming transitions in force-based models for pedestrian dynamics. *Phys. Rev. E*, 92:042809, 2015.

[60] M. Treiber and A. Kesting. *Traffic Flow Dynamics*. Springer, Berlin, 2013.

[61] Forschungszentrum Jülich and Wuppertal University `ped.fz-juelich.de/database`.

[62] M. Boltes. Software `PeTrack`, Forschungszentrum Jülich. `ped.fz-juelich.de/petrack` and M. Boltes M and A. Seyfried. Collecting pedestrian trajectories. *Neurocomputing* 100:127–133, 2013.

[63] A.-H. Olivier, R. Kulpa, J. Pettre, and A. Cretual. A step-by-step modeling, analysis and annotation of locomotion. *Comput. Animat. Virtual Worlds*, 22:421–433, 2011.

[64] S. P. Hoogendoorn, W. Daamen, and R. Landman. Microscopic calibration and validation of pedestrian models - Cross-comparison of models using experimental data. In N. Waldau, P. Gattermann, H. Knoflacher, and M. Schreckenberg, editors, *Pedestrian and Evacuation Dynamics 2005*, pages 329–340. Springer Berlin Heidelberg, 2007.

[65] A. Johansson. Constant-net-time as a key mechanism behind pedestrian flow dynamics. *Phys. Rev. E*, 80:026120, 2009.

[66] D.J. Higham. An algorithmic introduction to numerical simulation of stochastic differential equations. *SIAM Rev.*, 43(3):525–546, 2001.